

Hydrogen-induced dynamic slowdown of metallic glass-forming liquids

Jin-Ai Gao(高津爱), Hai-Shen Huang(黄海深), and Yong-Jun Lü(吕勇军)
Citation: Chin. Phys. B, 2021, 30 (**6**): 066301. DOI: 10.1088/1674-1056/abf111
Journal homepage: http://cpb.iphy.ac.cn; http://iopscience.iop.org/cpb

What follows is a list of articles you may be interested in

Surface-regulated triangular borophene as Dirac-like materials from density functional calculation investigation

Wenyu Fang(方文玉), Wenbin Kang(康文斌), Jun Zhao(赵军), Pengcheng Zhang(张鹏程)
Chin. Phys. B, 2020, 29 (**9**): 096301. DOI: 10.1088/1674-1056/ab9bff

Raman scattering study of two-dimensional magnetic van der Waals compound VI_3

Yi-Meng Wang(王艺朦), Shang-Jie Tian(田尚杰), Cheng-He Li(李承贺), Feng Jin(金峰), Jian-Ting Ji(籍建葶), He-Chang Lei(雷和畅), Qing-Ming Zhang(张清明)
Chin. Phys. B, 2020, 29 (**5**): 056301. DOI: 10.1088/1674-1056/ab8215

Raman scattering study of magnetic layered MPS_3 crystals (M=Mn, Fe, Ni)

Yi-Meng Wang(王艺朦), Jian-Feng Zhang(张建丰), Cheng-He Li(李承贺), Xiao-Li Ma(马肖莉), Jian-Ting Ji(籍建葶), Feng Jin(金峰), He-Chang Lei(雷和畅), Kai Liu(刘凯), Wei-Lu Zhang(张玮璐), Qing-Ming Zhang(张清明)
Chin. Phys. B, 2019, 28 (**5**): 056301. DOI: 10.1088/1674-1056/28/5/056301

Unconventional lattice dynamics in few-layer h-BN and indium iodide crystals

Gan Hu(胡干), Jian-Qi Huang(黄建啟), Ya-Ning Wang(王雅宁), Teng Yang(杨腾), Bao-Juan Dong(董宝娟), Ji-Zhang Wang(王吉章), Bo Zhao(赵波), Sajjad Ali(阿里·萨贾德), Zhi-Dong Zhang(张志东)
Chin. Phys. B, 2018, 27 (**8**): 086301. DOI: 10.1088/1674-1056/27/8/086301

First-principles analysis of the structural, electronic, and elastic properties of cubic organic-inorganic perovskite $HC(NH_2)_2PbI_3$

Jun-Fei Wang(王俊斐), Xiao-Nan Fu(富笑男), Jun-Tao Wang(王俊涛)
Chin. Phys. B, 2017, 26 (**10**): 106301. DOI: 10.1088/1674-1056/26/10/106301

Hydrogen-induced dynamic slowdown of metallic glass-forming liquids*

Jin-Ai Gao(高津爱), Hai-Shen Huang(黄海深), and Yong-Jun Lü(吕勇军)†

School of Physics, Beijing Institute of Technology, Beijing 100081, *China*

(Received 30 January 2021; revised manuscript received 15 March 2021; accepted manuscript online 23 March 2021)

Dynamics of hydrogen doped $Cu_{50}Zr_{50}$ glass-forming liquids are investigated by using the newly developed modified embedded atomic method (MEAM) potential based on molecular dynamics simulations. We find that the doping of hydrogen atoms slows down the relaxation dynamics, reduces the fragility of supercooled melts, and promotes the occurrence of glass transitions. The dynamic slowdown is suggested to be closely related to the effect of hydrogen atoms on locally ordered structure of melts. With increasing concentration of hydrogen, the five-fold symmetry associated with Cu- and Zr-centered polyhedrons is lowered, on the other hand, the local order featuring metal hydrides is enhanced. The latter dominates the dynamic behaviors of glass-forming liquids, especially for Zr atoms, and results in the dynamic slowdown.

Keywords: metallic glasses, hydrogen, dynamics

PACS: 63.50.Lm, 64.70.pe, 62.20.mj **DOI:** 10.1088/1674-1056/abf111

1. Introduction

Metallic glasses have potential application in the fields of hydrogen storage and biomaterials.[1,2] Understanding the influence of hydrogen on the properties of metallic glasses is of importance for optimizing the performance of the materials. Experimental and simulation studies have shown that the hydrogen microalloying has beneficial effect on glass-forming ability (GFA) and mechanical properties of bulk metallic glasses (BMG). For example, both GFA and malleability of Zr-based BMG are improved by doping hydrogen due to strong binding to Zr.[3,4] In contrast, Pd-based BMG shows low hydrogen affinity and thus the effect of hydrogen doping is less significant.[5] *Ab initio* molecular dynamics (MD) simulations have revealed that a small addition of H atoms can decrease the icosahedral order and slow down the atomic mobility in CuZrAl glass.[6] Experimental results argued that more large free volume regions collapse by the addition of hydrogen and the denser random packed structure is formed, thus enhancing GFA.[7] In addition, the doping of hydrogen was found to enhance the diversity of locally ordered structures, which was believed to be responsible for the improved ductility.[8] In fact, the performance modification of metallic glasses via hydrogen doping largely depends on the concentration of hydrogen. With increasing addition of hydrogen, the thermal stability of metallic glasses inevitably becomes poor, ultimately leading to crystallization. The amorphous Cu–Zr alloy has been proved to be decomposed into a mixture of crystalline phase Cu, Cu_xZr_y compound and ZrH_2 at high temperature and high hydrogen pressure.[9] In most cases, the effect of hydrogen has been involved in the preparation stage of metals, where the melts are quenched in the protective atmosphere composed of a small amount of hydrogen as reductant.[10,11] The effect of hydrogen doping on properties of supercooled glass-forming liquids therefore should be clarified first. In this work, we optimize the potential parameters of Cu/Zr/H system within the framework of modified embedded atomic method (MEAM). Based on the interatomic potential, we study the dynamic properties of hydrogen doped $Cu_{50}Zr_{50}$ glass-forming liquids using MD simulations, and reveal the structural origin of hydrogen-induced dynamic slowdown.

2. Computational methods

2.1. MEAM potential for Cu/Zr/H system

We use the MEAM potential to describe the interactions between hydrogen and metallic base in MD simulaitons. This model was first proposed by Baskes *et al*. In the MEAM, the total energy of a system is approximated as a sum of the pairwise interaction and the embedding energy as a function of background electron density by taking the bonding directionality into consideration.[12,13] For liquid systems, the MEAM potential shows a good application provided appropriate parameters or functional forms. Also, the MEAM potential is capable of describing the bonding characteristic of hydrogen and metallic elements, thus it is preferred in this work. Lee *et al.* developed an original version of the MEAM potential for Cu/Zr/H system.[14,15] The calculations based on their parameters show that the energies of Cu–Zr as well as the diffusion of hydrogen are not sufficiently accurate. Therefore, at first, we optimized the MEAM parameters based on Lee's work. The

*Project supported by the National Natural Science Foundation of China (Grant No. 52071029). The computer resources at the Shanghai and Tianjin Supercomputer Centers are gratefully acknowledged.

†Corresponding author. E-mail: yongjunlv@bit.edu.cn

© 2021 Chinese Physical Society and IOP Publishing Ltd

present training set is composed of several Cu–Zr compounds and Cu and Zr hydrides. We used the single parameter optimizer in training. Tables 1–3 provide the MEAM parameters for Cu/Zr/H developed in this work.

Table 1. 2NN MEAM potential parameters sets for pure Cu, Zr, and H.

	$C_{\min}$	$C_{\max}$	ρ_0
Cu	0.20	2.80	1.0
Zr	0.20	2.80	1.2
H	0.20	2.80	16.0

Table 2. 2NN MEAM potential parameters for the binary *M*–*M* and *M*–H (*M* = Cu, Zr) systems.

Type	Cu–Zr	Cu–H	Zr–H
Reference state	CuZr(B2)	CuH(B3)	ZrH(B3)
δ	0.12	–0.1	–0.15
α	4.9021	3.9046	3.3858
E_c	4.830	3.055	4.515
r_e	2.8162	1.90	1.85
$C_{\min}$(A,A,B)	0.2	0.74	2
$C_{\min}$(B,B,A)	0.2	0.09	0.09
$C_{\min}$(A,B,A)	0.2	0.64	0.5
$C_{\min}$(B,A,B)	0.2	0.35	2
$C_{\max}$(A,A,B)	2.8	2.8	2.8
$C_{\max}$(B,B,A)	2.8	1.44	1.44
$C_{\max}$(A,B,A)	2.8	2.8	2.15
$C_{\max}$(B,A,B)	2.8	2.8	2.8

Table 3. Parameter sets of $C_{\min}$ and $C_{\max}$ for Cu–Zr–H system.

Type	Cu–Zr–H	Cu–H–Zr	H–Zr–Cu
$C_{\min}$	1.29	0.57	1.29
$C_{\max}$	2.80	2.46	2.80

We first check the application of the present MEAM potential in describing the energy and structure of Cu–Zr systems. Here, the embedded atomic method (EAM) potential[16] for Cu–Zr alloys developed by Mendelev *et al.* is used as a reference, which has been proved to have high accuracy in reproducing various properties of Cu–Zr liquids and glasses. Figure 1 shows that the present MEAM potential well predicts the potential energies of $Cu_{50}Zr_{50}$ over the range from high-temperature liquid state to glass state compared to the results from reported MEAM potentials. Based on the temperature dependence of the potential energies, our model predicts that the glass transition occurs at $T = 733$ K, which is much close to the value of $T = 736$ K by the EAM potential and better than the result of $T = 768$ K predicted by Lee's potential. Table 4 provides the comparison of the nearest neighboring distance in $Cu_{50}Zr_{50}$ glass. The value for Cu–Zr pair predicted by our model potential is more consistent with the experimental and EAM results. We further check the diffusion coefficients of hydrogen in face-centered cubic (fcc) Cu and body-centered cubic/hexagonal close-packed (bcc/hcp) Zr by referring to experimental data. The results shown in Fig. 2 indicate that the present MEAM parameters have a better application of predicting hydrogen dynamics. The above comparisons confirm that the MEAM potential developed in this work can more reasonably describe the interactions among Cu, Zr, and H, especially in liquid and glassy states.

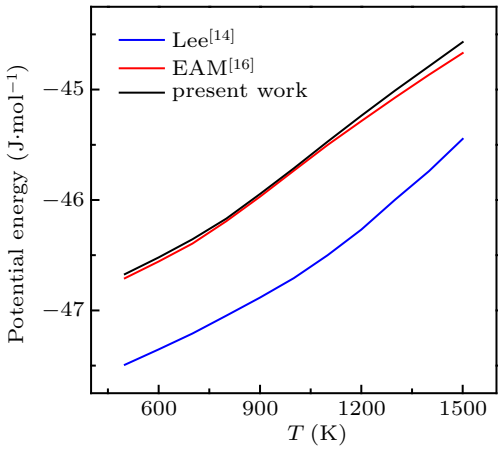


Fig. 1. Comparisons of potential energies of $Cu_{50}Zr_{50}$ between MEAM and EAM potentials.

Table 4. Nearest neighboring distances of Cu–Cu, Zr–Zr, and Cu–Zr pairs in $Cu_{50}Zr_{50}$ glass at $T = 300$ K.

	EAM[16]	MEAM-Lee[14]	Expt. (XRD)[17]	Present work
Cu–Cu	2.55	2.45	2.53	2.45
Cu–Zr	2.75	2.95	2.75	2.85
Zr–Zr	3.25	3.15	3.15	3.15

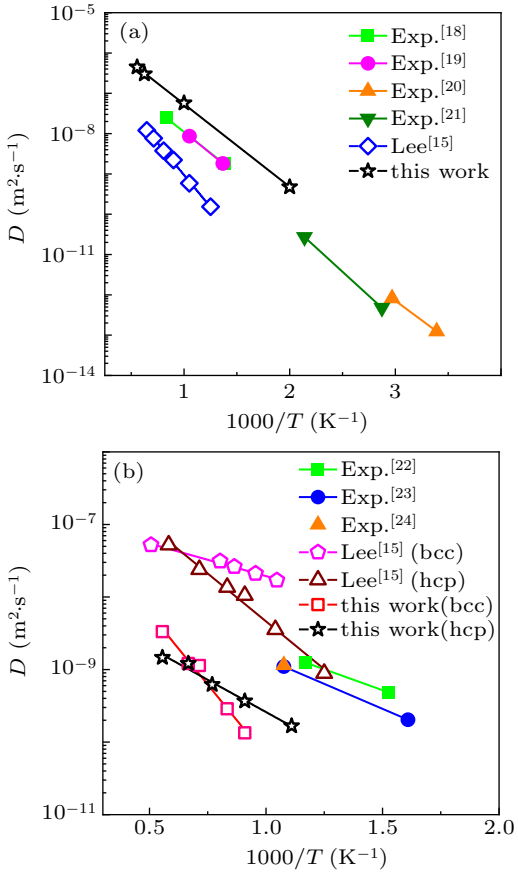


Fig. 2. Self-diffusion coefficients of hydrogen atom in (a) fcc Cu and (b) bcc/hcp Zr predicted by MEAM potentials in comparison with experimental data.

2.2. MD simulations

The quenching processes of $(Cu_{50}Zr_{50})_{100-x}H_x$ ($x = 0$–10) were simulated by using MD simulations based on the newly developed MEAM potential. The systems consisting of 10976 atoms were equilibrated at 1800 K and then quenched to 500 K at zero pressure with a cooling rate of 0.1 K/ps, i.e., a relaxation of 1 ns every 100 K. The MD simulations were performed in the isothermal and isobaric ensemble (NPT) with the periodic boundary condition along the three dimensions and a time step of 0.25 fs was used.

3. Results and discussion

3.1. Dynamic properties of $(Cu_{50}Zr_{50})_{100-x}H_x$ system

For the H-free $Cu_{50}Zr_{50}$ melt, the calorimetric glass transition temperature T_g is 733 K under the present simulation conditions. The addition of H is found to universally increase T_g to 800 ± 10 K. Clearly, the melt is more easily quenched into glassy state with hydrogen, which is consistent with the experimental results of CuZrNiAl alloy.[7] We analyze the relaxation dynamics of supercooled melts by calculating the intermediate self-scattering function (ISF)

$$F_s(q,t) = \frac{1}{N}\left\langle \sum_{j=1}^{N} \exp\{i\boldsymbol{q}\cdot[\boldsymbol{r}_j(t) - \boldsymbol{r}_j(0)]\}\right\rangle, \quad (1)$$

where $\boldsymbol{q}$ is the wave vector, and $|q| = 2.688$ Å^{-1} corresponding to the first peak of the static structure factor. The structural relaxation time τ_α is estimated by the time decaying to $1/e$.[25] Figure 3 shows the logarithm plot of the relaxation time as a function of the inverse of temperature upon approaching glass transition. The relaxation is shown to be slowed down by doping H atoms, and moreover, it is more pronounced with increasing concentration of H. All the temperature dependences of relaxation time obey the Vogel–Fulcher–Tamman law (VFT)[26] $\tau_\alpha = \tau_0 \exp[D_T T_0/(T - T_0)]$. However, the fitted values of the parameter D_T increase from 0.877 for the H-free, 1.028 for 2 at.% H to 1.211 for 8 at.% H. It means that the supercooled liquid becomes stronger with more H atoms.

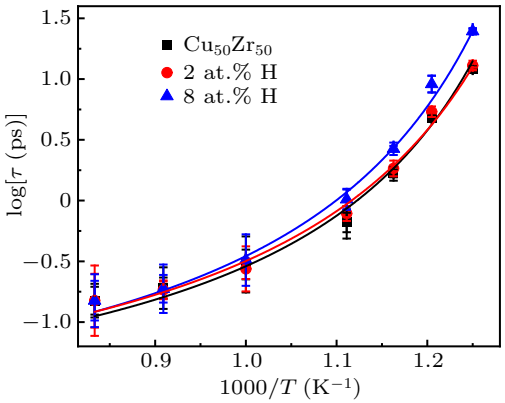


Fig. 3. Logarithm relaxation time as a function of the inverse of temperature, and the solid lines are fits to VFT law.

The fragility of supercooled liquids can also be measured from a thermodynamic point of view. We calculate the specific heat C_p in the NPT ensemble through glass transition. In general, the abrupt decrease of specific heat across glass transition varies with the fragility of supercooled glass-forming liquids: considerable changes in stronger glass formers but small ones in fragile formers like GeO_2.[27,28] Figure 4 shows that ΔC_p rises significantly with increasing content of H, from 9.170 J·mol^{-1}·K^{-1} to 10.629 J·mol^{-1}·K^{-1} for 2 at.% and 14.128 J·mol^{-1}·K^{-1} for 8 at.%. It indicates that the liquid becomes stronger as more H atoms are added, which is consistent with the results from the dynamic fragility in Fig. 3. On the other hand, the contribution of the thermal motion of H atoms is ignorable considering its very small amount, thus, the rise of ΔC_p actually implies that the addition of H atoms induces more complex atomic motions of base elements.

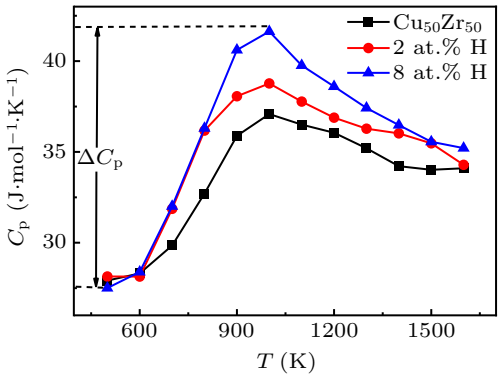


Fig. 4. Specific heat as a function of temperature at different concentrations of hydrogen across glass transitions.

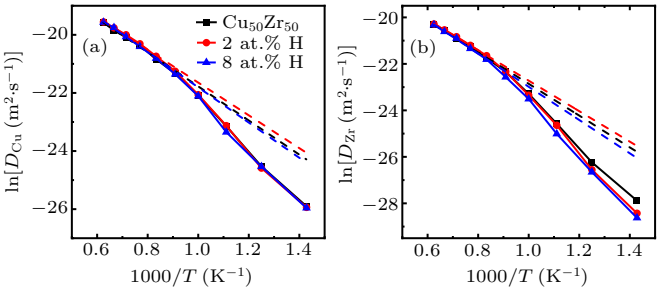


Fig. 5. Logarithm plots of diffusion coefficients of $(Cu_{50}Zr_{50})_{1-x}H_x$ ($x = 0$, 2, 8) as a function of the inverse of temperature. (a) Cu and (b) Zr. The dashed lines are fits to the Arrhenius relation.

Figure 3 reflects the slowdown of the overall structural relaxation. To clarify the chemical dependence of the dynamic slowdown, we calculate the self-diffusion coefficients of Cu and Zr during quenching, respectively, which is given by the long-time limit of the mean squared displacements[29]

$$D = \lim_{t\to\infty} \frac{1}{6Nt} \sum_{j=1}^{N} [\boldsymbol{r}_j(t) - \boldsymbol{r}_j(0)]^2. \quad (2)$$

Figure 5(a) shows that the diffusion of Cu atoms is not markedly influenced by the addition of H atoms. The Cu diffusion coefficients in both H-free and H-doped systems display

approximately the same super-Arrhenius temperature dependence. In contrast, the diffusion coefficients of Zr atoms have a distinct decrease with increasing content of H, displaying a growing deviation from the Arrhenius relation, as shown in Fig. 5(b). It is clear that the dynamic slowdown of $Cu_{50}Zr_{50}$ melts is mainly contributed by more sluggish Zr atoms due to the doping of H. In short, the addition of H atoms is able to slow down the diffusion, relaxation process of base melts and make the system stronger.

3.2. Structural characteristics of $(Cu_{50}Zr_{50})_{100-x}H_x$ melts

We aim to reveal the structural origin of the slowdown dynamics. We analyze the local structure of supercooled liquids using the Voronoi polyhedron method. For glassy systems, icosahedrons were believed to be of importance in featuring local structure, and therefore were often taken as the characteristic quantity to understand the relation between structure and dynamic properties.[30] More general, the dynamic properties were found to be closely related to the local five-fold symmetry associated with Voronoi polyhedron,[31] which is defined as $W = \sum_i (f_i^5 \times P_i)$, where f_i^5 represents the proportion of pentagons, $f_i^5 = n_i^5 / \sum_i n_i^k$, n_i^k ($k = 3, 4, 5, 6$) is the number of k-side polygons in Voronoi polyhedron i, and P_i is the fraction of Voronoi polyhedron i. We count the number of various polyhedrons in supercooled liquids, and find that the polyhedrons with high five-fold symmetry rank in the top ones regardless of the addition of H atoms. It is consistent with the locally structural characteristics of metallic glasses, whereas the fractions of these polyhedrons have a overall decrease with increasing content of H. Figure 6 presents the average five-fold symmetry in the melts as a function of temperature. It shows a distinct decrease as more H atoms are doped. These results indicate that H atoms tend to decompose the local five-fold symmetry structure, which agrees with the reported *ab initio* simulations.[7] The five-fold symmetry structure was argued to facilitate the glass transition due to the frustration of crystallization.[32] Obviously, its reduction is contradictory to the fact that the glass transition is enhanced in the present simulations. In addition, we find that the high five-fold symmetry polyhedrons are not decomposed into denser packing structure. Figure 7(a) shows that the average atomic volume V actually is increased by doping H atoms. It suggests that H atoms segregate in interstices of polyhedrons and result in the expansion of atomic volumes for both Cu and Zr, forming more large-volume polyhedrons. Such volume expansion is relatively weak and does not significantly change the global structure of the base alloys, as evidenced by the radial distribution functions (RDFs) for Cu–Zr, Cu–Cu, and Zr–Zr pairs shown in Fig. 7(b). Although that, Fig. 4 clearly shows that the atomic mobility is slowed down. Therefore, more intrinsic structural cause is needed to resolve these contradictions.

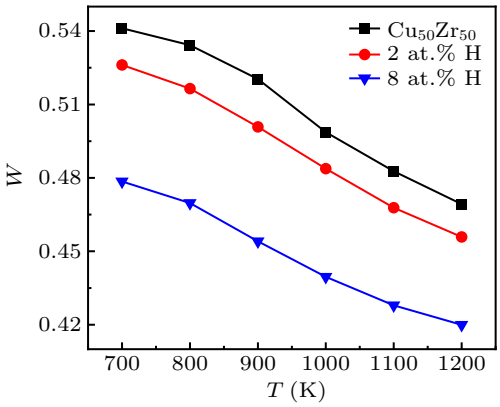


Fig. 6. Average five-fold local symmetry of $(Cu_{50}Zr_{50})_{1-x}H_x$ ($x = 0$, 2, 8) versus temperature.

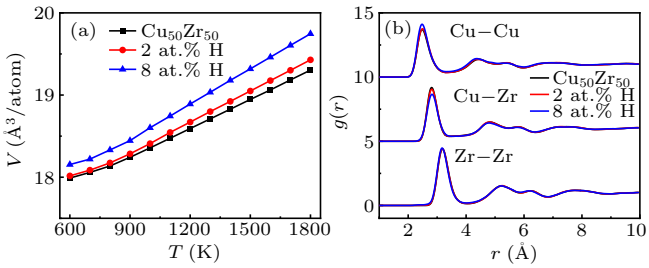


Fig. 7. (a) Average atomic volume as a function of temperature for H-free, 2 at.% and 8 at.% H systems. (b) Partial RDFs of Cu–Zr, Cu–Cu, and Zr–Zr pairs at $T = 500$ K.

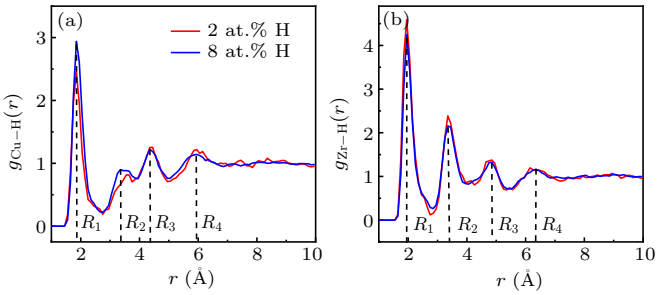


Fig. 8. Partial radial distribution functions of $(Cu_{50}Zr_{50})_{1-x}H_x$ ($x = 2$, 8) at 500 K. (a) Cu–H pair and (b) Zr–H pair.

Experimental and numerical studies have found that the relative peak positions in RDFs of metallic glasses are identical with the values of their crystalline counterparts, which suggests that disordered systems may hide the translational order inherited from crystal phases.[31,32] It is possible that there is a competition between the five-fold symmetry and the crystalline ordering in metallic glasses. To some extent H atoms tend to bond to base elements, forming metal hydrides, in particular with Zr atoms. We explore this possibility by means of RDFs. Figure 8 shows the partial RDFs of Cu–H and Zr–H pairs. We calculate the peak positions relative to the nearest neighboring distance, and compare them with several typical hydride compounds.[33,34] We find that the second, third, and forth relative peak positions of Zr–H pairs have a good

match with those of ZrH_3;[35] comparatively, for Cu–H pairs, the second and third relative peaks match with those of CuH compound but a bit large deviation is found in the forth peak position, as listed in Table 5. The translational order associated with crystal phases indeed exists between H and metallic components, especially between Zr and H. To further reveal the hidden ordering, the bond angle distributions around Zr atoms are provided in Fig. 9.[36]

Table 5. Ratios of the second, third, and fourth peak positions in RDF to the nearest neighboring distance for Cu–H and Zr–H pairs.

		R_2/R_1	R_3/R_1	R_3/R_1
Cu–H	CuH	1.92	2.32	2.51
	CuZrH (2 at.% H)	1.92	2.40	3.22
	CuZrH (8 at.% H)	1.81	2.35	3.22
Zr–H	ZrH_3	1.73	2.24	3.00
	CuZrH (2 at.% H)	1.72	2.49	3.15
	CuZrH (8 at.% H)	1.72	2.49	3.27

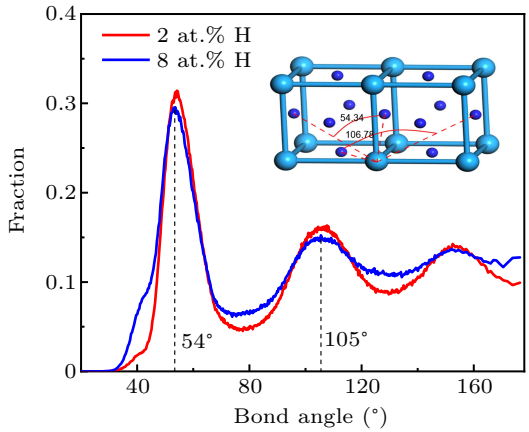


Fig. 9. Distributions of bond angle centering Zr atoms in supercooled CuZrH liquids at $T = 700$ K. The inset schematically illustrates the structure of ZrH_3 compound. The cyan and blue balls denote Zr and H atoms.

The bond angle at the first peak well corresponds to the value of ∠HZrH ($\sim 54°$) in the nearest neighboring distance of ZrH_3, and the one at the second peak corresponds to the ∠HZrH in the second nearest neighboring distance of ZrH_3 ($\sim 106°$). Therefore, the orientational order also exists between H and Zr. In fact, ZrH_3 has stronger cohesive energy among Zr hydrides, and it is more stable at high H-concentration. The tendency of forming ordered bonds between Zr and H induces the slowdown of Zr mobility, despite that the atomic volume is expanded. Meanwhile, we analyze the spatial distribution of H atoms and find that more H atoms segregate around Zr atoms with decreasing temperature, for example, exceeding 60% in 2 at.% system at 800 K. Therefore, the interactions between Zr and H play a primary role in H-induced dynamics. The addition of H atoms destroys the high five-fold symmetry polyhedron, and on the other hand, the bonding between Zr and H slows down the dynamics. The tradeoff between them determines the dynamic behavior and thermal stability. In the case of small addition of H atoms, the latter is dominant and the dynamics of the melts becomes slow. Furthermore, due to the ordered bonding, more thermal motion modes are expected in the base metals, which provides an explanation for the increasing ΔC_p across glass transition with increasing H content. In simulations, we increase the concentration of H up to 10 at.% and find that more H atoms tend to segregate, which will inevitably influence the phase stability. If the H concentration is further increased, the crystallization of metallic hydrides is expected to occur.

4. Conclusion

In summary, we optimize the MEAM potential parameters of Cu/Zr/H system. The newly developed parameters show a better application of describing the structure and dynamic properties of Cu/Zr/H system. Based on the potential, we use MD simulations to study the dynamics of H doped $Cu_{50}Zr_{50}$ liquid. The results reveal that the doping of H atoms in the supercooled glass-forming liquid induces the slowdown of structural relaxation and stronger liquid state. The dynamic changes are closely related to the interplay between H and Zr atoms. Structural analyses indicate that the local five-fold symmetry is reduced by adding H and ordered bonding between Zr and H is enhanced. The latter is the dominant cause for the slow dynamics and the enhanced glass transition. This work is helpful to comprehensively understand the dynamics of H-metallic glass systems as well as its structural origin.

References

[1] Ciureanu M 1993 *J. Electrochem. Soc.* **140** 579
[2] Hu Y C, Wang Y Z, Su R, *et al.* 2016 *Adv. Mater.* **28** 10293
[3] Dong F Y, Su Y Q, Luo L S, Wang L, Wang S J, Guo J J and Fu H Z 2012 *Int. J. Hydrogen Energy* **37** 14697
[4] Gebert A, Ismail N, Wolff U, Uhlemann M, Eckert J and Schultz L 2002 *Intermetallics* **10** 1207
[5] Granata D, Fischer E and Löffler J F 2015 *Acta. Mater.* **99** 415
[6] Mahjoub R, Laws K J, Hamilton N E, Granata D and Ferry M 2016 *Comp. Mater. Sci.* **125** 197
[7] Su Y Q, Dong F Y, Luo L S, Guo J J, Han B S, Li Z X, Wang B Y and Fu H Z 2012 *J. Non-Cryst. Solids.* **358** 2606
[8] Eliaz N and Eliezer D 1999 *Adv. Perform. Mater.* **6** 5
[9] Katona T, Molnár Á, Perczel I V, Kopasz C and Hegedüs Z 1992 *Surf. Interface Anal.* **19** 519
[10] Zheng C H, Wang H P, Zou P F, Hu L and Wei B 2020 *Metall. Mater. Trans. A* **51** 4074
[11] Lü P, Wang H P, Zou P F, Zhou K, Hu L and Wei B 2018 *J. Appl. Phys.* **124** 025103
[12] Baskes M I, Nelson J S and Wright A F 1989 *Phys. Rev. B* **40** 6085
[13] Baskes M I 1992 *Phys. Rev. B* **46** 2727
[14] Kim Y M and Lee B J 2008 *J. Mater. Res.* **23** 1095
[15] Lee B M and Lee B J 2014 *Metall. Mater. Trans. A* **45** 2906
[16] Mendelev M I, Sordelet D J and Kramer M J 2007 *J. Appl. Phys.* **102** 043501
[17] Chen H S and Waseda Y 1979 *Phys. Status Solidi* **51** 593
[18] Katz L, Guinan M and Borg R J 1971 *Phys. Rev. B* **4** 330
[19] Bugeat J P and Ligeon E 1979 *Phys. Lett. A* **71** 93
[20] Sakamoto Y and Takao K 1982 *J. Jpn. Inst. Met* **46** 285
[21] Ishikawa T and McLellan R B 1985 *J. Phys. Chem. Solids.* **46** 445
[22] Schwartz C M and Mallett M W 1954 *Trans. ASM* **46** 640
[23] Mallett M W and Albrecht W M 1957 *J. Electrochem. Soc.* **104** 142

[24] Mazzolai F M and Ryll-Nardzewski J 1976 *J. Less-Common Met.* **49** 323
[25] Cheng Y, Wang Y Y, Peng C X, Zhang Z T, Wang P F, Jia L J, Li X L and Wang L 2019 *J. Alloys Compd.* **786** 627
[26] Cao Q L, Huang D H, Yang J S and Wang F H 2020 *Chin. Phys. Lett.* **37** 076201
[27] Angell C A 1995 *Science* **267** 1924
[28] Brüning R and Crowell T 1999 *J. Non-Cryst. Solids.* **248** 183
[29] Bi Q L and Lü Y J 2014 *Chin. Phys. Lett.* **31** 106401
[30] Yeh X L, Samwer K and Johnson W L 1983 *Appl. Phys. Lett.* **42** 242
[31] Gao W, Feng S D, Qi L, Zhang S L and Liu R P 2015 *Chin. Phys. Lett.* **32** 116101
[32] Hu Y C, Li F X, Li M Z, Bai H Y and Wang W H 2015 *Nat. Commun.* **6** 8310
[33] Liu X J, Xu Y, Hui X, Lu Z P, Li F, Chen G L, Lu J and Liu C T 2010 *Phys. Rev. Lett.* **105** 155501
[34] Wu Z W, Li M Z, Wang W H and Liu K X 2015 *Nat. Commun.* **6** 6035
[35] Persson K 2016 *Materials Project*
[36] Lü Y J and Entel P 2011 *Phys. Rev. B* **84** 104203